OPTIMIZATION OF THE DESIGN OF EDDY CURRENT PROBE OF PARAMETRIC TYPE TO DETECT SURFACE CRACKS

V.M. Uchanin

G.V. Karpenko Physico-Mechanical Institute of the NASU
5 Naukova Str., 79060, Lviv, Ukraine

ABSTRACT

The paper summarizes the results of research concerned with optimization of the eddy current probe of the parametric type used for surface defects detection. It is shown that the choice of eddy current probe diameter significantly depends on the smallest length of cracks needed to be detected. In particular, it was determined that to detect a crack longer than 2 mm, it is optimal to use an eddy current probe with windings mounted on the 1.2 mm diameter ferrite core. To detect shorter cracks longer than 1 mm, it is necessary to use an eddy current probe with windings on the 0.75 mm diameter ferrite core. The influence of ferrite core parameters (length, magnetic permeability, and offset of winding from the ferrite core end) on the efficiency of parametric type eddy current probes is analyzed. The results obtained should be used for eddy current probe optimization. The conditions of separation of defect and lift-off influence are analyzed by interpretation of signals in the complex plane, and the possibility of their separation for the developed eddy current probes for all nonmagnetic structural alloys is shown. The design of a parametric type eddy current probe makes it possible to increase their quality factor more than twice. The optimal choice of the cable for connection of an eddy current probe and flaw detector is considered. The optimized parametric eddy current probes were tested. The high sensitivity of the developed probe to short cracks longer than 2 mm with reliable separation of the defect and lift-off influence was shown.

KEYWORDS: eddy current non-destructive testing, surface crack, eddy current probe, ferrite core

INTRODUCTION AND PROBLEM STATUS

Over the recent decades the eddy current method has taken up a leading position among the most widely accepted NDT methods, which ensure detection of surface defects (for instance, fatigue cracks) in metal structures without contact with the controlled surface or even through a dielectric coating [1–9]. We will note as a no-alternative example that only miniature eddy current probes (ECP) may reliably detect cracks in difficult-of-access places of aircraft structures, in particular those located on the side wall of rivet holes, where cracks usually form because of mechanical stress concentration [1, 7]. At the same time, eddy current flaw detection methods are sensitive to a range of factors (in addition to defects), which essentially influence the ECP output signal. These factors include changes in electric conductivity and magnetic permeability of the studied material, variations of the geometrical parameters, or lift-off between ECP and surface of the evaluated object (EO). Experienced operators are looking for a possibility to remove or reduce this interference to obtain reliable control results. Changes of ECP lift-off or inclination are especially critical for manual eddy current evaluation, when ECP position relative to EO changes during scanning. Changes in the lift-off due to different roughness of EO surface, or a change in dielectric coating thickness, can also lead to wrong decisions about presence of defects. Therefore, it is important to reduce the in-

fluence of the lift-off for a reliable detection of defects. It is usually difficult to reveal short (even deep) defects in the structures, such as corrosion pits and shallow (even long) cracks. That is why development of testing technologies is aimed at improvement of the possibilities for detection of short and shallow defects with high reliability based on reducing the influence of interference of different physical nature. The reliability of control is used to assess the probability of defect detection, as a qualitative parameter based on statistics. Even for one and the same equipment the probability of defect detection is influenced by several factors, such as EO materials properties, defect type and dimensions, testing conditions, etc.

Important components of the procedure for surface crack detection is selection of ECP type and geometrical parameters for reliable detection of cracks, the dimensions of which characterize the sensitivity threshold, and simple interpretation of the signal that allows separation of useful signals, generated by cracks, from those related to such factors as lift-off or influence of the edge [1, 5, 7, 9]. For the majority of eddy current testing procedures, it is believed to be enough to reliably detect more than 2 mm long and more than 0.2 mm deep cracks that determines the sensitivity threshold of eddy current flaw detectors (ECFD). Such a defect should be reliably detected through a dielectric coating up to 0.5 mm thick. In this case, structural elements protected by anticorrosion coating will be evaluated without a costly procedure of its re-

moval. However, for testing aircraft engine components, an attractive goal is the possibility to detect two times shorter cracks (about 1 mm), for which the eddy current technique can also be used in principle, under the condition of correct selection of ECP parameters.

In works [1–8] different types of ECP were considered and analyzed, which can be used to detect surface cracks. To detect short surface cracks in manual scanning mode, it is the most convenient to use the simplest ECP with one single-layer winding, mounted on a cylindrical ferrite core (FC) [1, 8, 10–13]. An important advantage of such an ECP is the independence of its sensitivity on the crack direction that allows selection of arbitrary scanning paths without the need to maintain ECP orientation relative to the direction of the probable crack. Not less important features of parametric ECP, influencing such a choice, are design simplicity, small size, ease of meeting the requirements as to parameter repeatability in manufacture and low cost [1, 7, 8, 10–11]. Such ECP are traditionally used in self-generator ECFD [8]. More over, single-winding ECP are applied in ECFD operating in resonance mode, the most widely spread of which are known ECFD of DEFECTOMETR family (for instance, DEFCTOMETR 2.837), developed in Germany by Institute Dr. Foerster GmbH&Co). In some all-purpose ECFD, for instance of EDDYCON type, produced by SPC "Promprylad" (Ukraine), or ECFD of ELOTEST M2 type of Rohmann GmbH (Germany), the resonance mode is used as an auxiliary one.

Known is the traditional approach to determination of ECP efficiency, when the surface of a standard specimen (SS) with a defect is scanned and the ECP output signal from the defect is monitored. ECP efficiency is determined by the parameters of the signal from the defect, in particular, its amplitude. Such a procedure is usually used during selection of optimal ECP and working frequency to solve a specific flaw detection task [1, 8, 14]. Such a practice was also envisaged by the European standard on determination of ECP characteristics [15]. With such an approach, it is difficult to compare the results of efficiency evaluation performed by different researchers, as the experiment conditions should be reproduced. In particular, for SS manufacture, it is necessary to use a material with identical electrophysical characteristics and introduce a defect of identical dimensions. A method to determine ECP efficiency, presented by the American Bureau of Standards in works [16, 17], is more advanced. With this method, ECP impedance is measured when it is placed at a distance from SS (in "air") and when mounted on the surface of aluminium SS. ECP efficiency is evaluated by the difference in measured impedances. A disadvantage of this method

is its dependence on the selected operational frequency, resonance frequency and number of ECP winding turns that limits its application for determination of ECP design efficiency, irrespective of the number of turns and test working frequency.

For quantitative evaluation of the influence of different structural factors on ECP efficiency, it was proposed to use a dimensionless coefficient of eddy current efficiency ξ (Uchanin V.M. Method to determine the efficiency of eddy current probes. Patent of Ukraine 105072, 2014, Bull. No.4). Conditions necessary for studying it were also determined, and invariant properties of the coefficient of eddy current efficiency ξ for windings without FC were also determined, as regards winding diameter and turn number [18]. A procedure for calculation of ECP efficiency ξ was optimized for different ECP variants (also with FC) by the method of volume integral equations [12, 13, 19], using VIC-3D program [20].

This work is a generalization of the results of a number of investigations and developments, related to an optimal selection of structural and electrical parameters of the simplest ECP of parametric type, which are most often used to detect surface defects.

1. ENSURING THE SENSITIVITY THRESHOLD ALONG THE CRACK LENGTH BY SELECTION OF THE DIAMETER OF PARAMETRIC ECP WINDING

Selection of ECP winding diameter is determined by the length of the shortest crack to be detected. A nonoptimal selection of ECP dimensions may lead to overlooking critical defects or unjustified increase of time losses for testing. More over, analysis of the features of ECP signal for cracks of different length is required for interpretation of test results. When selecting the diameter of ECP winding, we will use the results of the work, in which the volume integral method is applied to study the spatial distribution of the signal generated by cracks of different length [9]. During modelling, the crack was located in the center of the system of coordinates: coordinate X corresponded to the direction transverse relative to the crack, coordinate Y ran in the direction along the crack. ECP winding parameters are as follows: average winding diameter D_{av}, winding thickness (difference between the outer and inner radius) Δr and winding height l_o. The signal from the crack was calculated in the form of introduced by the defect module Z_{cr} of ECP impedance, which was normalized to ECP impedance module Z_{eo}, when mounted in EO defectfree part : $Z'_{cr} = \Delta Z / Z_{eo}$. Crack length and ECP coordinates were normalized to average diameter of ECP winding: reduced crack length l_{cr}/D_{av}, reduced ECP coordinate along the crack $y' = yD_{av}$.
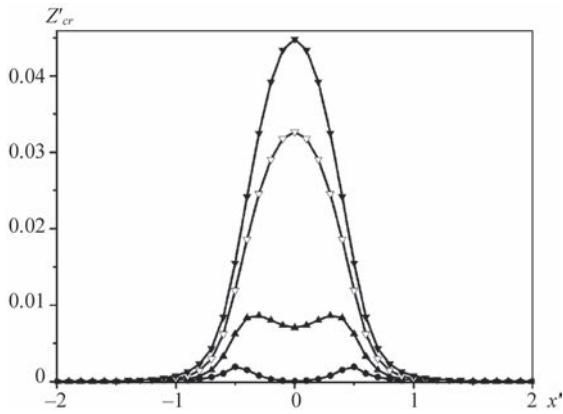
Figure 1. Changes of ECP signal during scanning with reduced lengths: ($\bullet$) — l'_{cr} = 0.3; ($\blacktriangle$) — l'_{cr} = 1.0; (∇) — l'_{cr} = 2.0; ($\blacktriangledown$) — l'_{cr} = 5.0

During development of eddy current testing procedures, information on the direction of possible propagation of cracks, which in real structures are determined by acting mechanical stresses, is often taken into account. It allows scanning in the direction transverse relative to the crack that corresponds to distribution of ECP signal amplitude along X coordinate (Figure 1), which was derived for scanning through the middle (y' = 0) of four cracks of different reduced length (l_{cr}' = 0.3; 1.0; 2.0 and 5.0). One can see that ECP signal dependence for short cracks (l'_{cr} < 0.3) has two maximums, and at ECP location over the center of such a crack (x' = 0), the signal can reach zero. However, with increase of crack length, the maximum amplitude value of the signal from the crack is observed exactly, when ECP is located directly over the defect (x' = 0). With such scanning, the maximum is

sufficiently "sharp", when ECP signal from the defect at a short distance, which is close to one diameter of ECP winding, rises abruptly to a maximum, and drops as rapidly after the maximum is passed. Such a feature allows the flaw detector operator reliably separating the signal from the defect from possible interference, the influence of which leads to slower changes of the signal during scanning. This feature is exactly responsible for certain advantages of such a scanning.

Figure 4 gives the distributions of ECP signals during scanning along the crack length by axis Y under the condition of preservation of ECP central position relative to the crack mid-plane. Note that the maximums of ECP signal during performance of an ordered transverse scanning in different crack sections (at different y coordinates) will also form a profile, similar to the distributions in Figure 2. Derived dependencies allow studying at which ECP position relative to the crack we have maximum signal values and possible sensitivity "dips" ("dead" zones).

Analysis of the obtained distributions (Figure 2) shows their essential dependence on the ratio of crack length to ECP diameter, i.e to the reduced crack length l'_{cr}. Here, not only the amplitude characteristics of ECP signals, but also the general view of signal distributions, change. This encourages us to analyze them separately.

To begin with, we will consider the most interesting case of short cracks, which we will conditionally assume to be cracks of reduced length l'_{cr} < 1.2. For short cracks distribution of ECP signal is of a two-hump symmetrical shape with the minimum at ECP
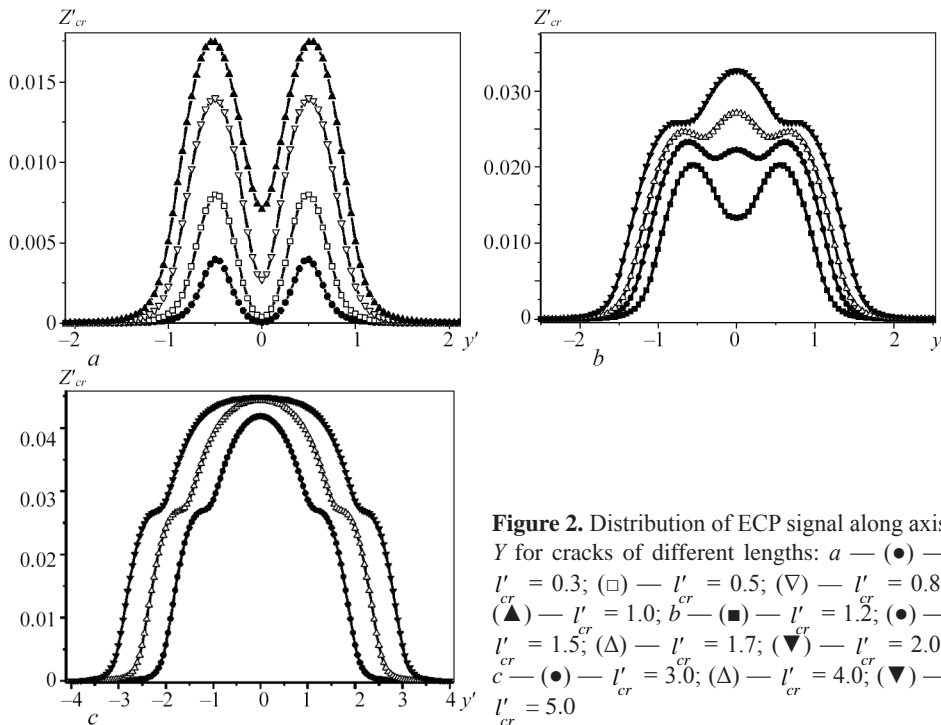
Figure 2. Distribution of ECP signal along axis Y for cracks of different lengths: a — ($\bullet$) — l'_{cr} = 0.3; ($\square$) — l'_{cr} = 0.5; (∇) — l'_{cr} = 0.8; ($\blacktriangle$) — l'_{cr} = 1.0; b — ($\blacksquare$) — l'_{cr} = 1.2; ($\bullet$) — l'_{cr} = 1.5; ($\triangle$) — l'_{cr} = 1.7; ($\blacktriangledown$) — l'_{cr} = 2.0; c — ($\bullet$) — l'_{cr} = 3.0; ($\triangle$) — l'_{cr} = 4.0; ($\blacktriangledown$) — l'_{cr} = 5.0

position directly over the crack (at $y = 0$). For a very short crack (relative to ECP dimensions), at $l'_{cr} < 0.3$ the amplitude can reach zero at crack location in the center of ECP winding. This is readily attributable to the features of distribution of ECP eddy current density, which is maximal directly over the winding turns, and fades to zero, when moving closer to ECP center (so-called "dead" zone), that is we have zero ECP signal in the case, when a short crack is located in the central "dead" zone of ECP and practically does not influence the eddy current redistribution. At the same time, ECP signal reaches its maximal value, when the crack middle is located directly under ECP windings, and has a maximal influence on eddy currents. Hence, it becomes clear that for short cracks with $l'_{cr} < 1.0$ the distance between the maximums is approximately equal to winding diameter D_{av}, and in the reduced coordinates in Figure 2, it is equal to 1.0. With increase of crack length, the distance between the maximums increases only slightly (see the distribution for $l'_{cr} = 1.2$ and 1.5 in Figure 2, *b*), and the values of signal amplitude in the minimum point become larger. At $l'_{cr} = 1.5$ the ECP signal distribution already has three maximums, as the central minimum begins to gradually transform into a maximum. With further increase of crack length, this maximum grows (see, for instance, signal changes for $l'_{cr} = 1.7$ in Figure 2, *b*).

At further increase of the crack length, ECP signal distribution has only one maximum, when ECP is located directly in the crack center with two symmetrical almost horizontal regions on both sides. It is important that increase of crack length, beginning from $l'_{cr} = 4.0$ already does not influence the signal amplitude in the central part of the distribution. With increase of reduced crack length l'_{cr}, the central maximum becomes broader, and a horizontal region forms (Figure 2, *c*). Established features of distribution of a signal from cracks of different length allowed suggesting a new method for determination of their length, invariant relative to the specified testing sensitivity (see Uchanin V.M. Eddy current method to determine the crack length. Patent of Ukraine 86505, 2009, Bull. No.3).

"Dips" in signal distribution in Figures 1 and 2, *a*, lead to the conclusion about the possibility of overlooking short cracks under the condition of incorrect selection of ECP diameter and scanning through the crack center. Here, misinterpretation of the results is also possible, as two maximums for a short crack can be taken as signals from two individual defects. Let us consider a physical explanation of the process of formation of the characteristic distribution of ECP signal
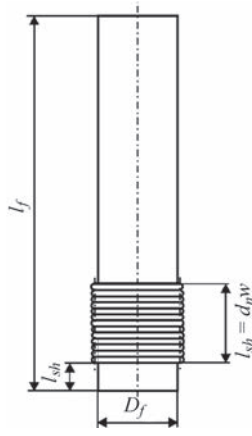
in the case of a crack of reduced length $l'_{cr} > 1.5$ (Figure 2, *b*). A gradual increase of signal amplitude begins at ECP movement into the crack zone. At further ECP displacement along the crack by axis *Y*, the beginning of the crack enters the "dead" zone, increase of ECP signal amplitude decelerates, and a horizontal region forms. Then the crack crosses the eddy current circuit from ECP other side, and further increase of the signal begins, which reaches a maximum directly over the defect. At further ECP movement, already the crack end falls within the "dead" zone, and another horizontal region forms.

The presented results were used to substantiate the dimensions of ECP for testing aircraft components, where the goal was to detect more than 2 mm long cracks [8]. For this purpose, the optimal ECP are those with windings, mounted on FC of 1.2 mm diameter that corresponds to a relatively uniform signal distribution for $l'_{cr} > 1.7$ in Figure 2, *b*. We will analyze parametric ECP with FC of such a diameter in greater detail in the next section from the view point of optimization of FC parameter selection. An ECP with a winding mounted on FC of 0.75 mm diameter was developed to detect short cracks of more than 1 mm length in aircraft engine parts.

2. OPTIMIZATION OF FERRITE CORE PARAMETERS OF PARAMETRIC ECP

Interaction of ECP turns with the material of the evaluated object (EO) is significantly reduced, depending on the distance from them to EO surface. Therefore, ECP geometry has an essential influence on its sensitivity [1, 16, 17]. FC application has the purpose of increasing the electromagnetic interaction of ECP upper turns with EO material. Therefore, optimal selection of the design of ECP with FC is an important stage of its development. Among the structural parameters of ECP with FC the most essential is FC diameter D_f and length l_f, winding length l_w (which for the single-layer winding is determined by the number of turns w and wire diameter d) and (offset) shifting l_{sh} of the winding relative to FC end (Figure 3).
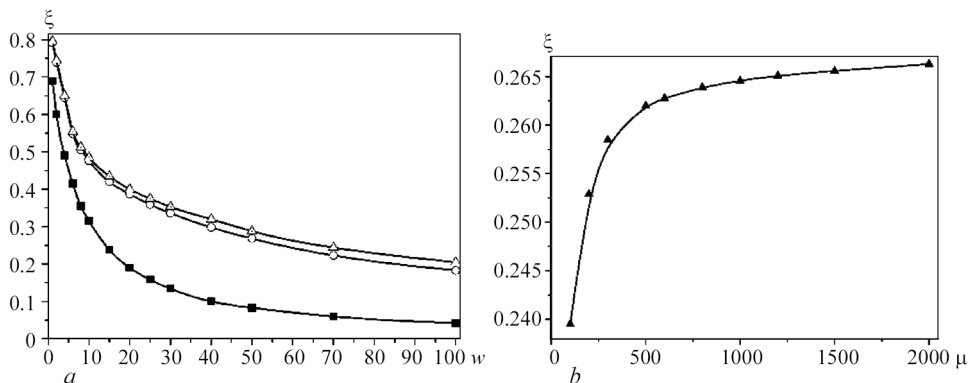
It is obvious that FC diameter D_f in most of the cases determines the diameter of ECP winding, selection of which was described in the previous section. All the other above-mentioned parameters of ECP with FC (Figure 3) influence the operation of parametric ECP in different ways. For quantitative evaluation of their influence we will use the given above coefficient of eddy current efficiency ξ (furtheron referred to as efficiency ξ). For parametric ECP with one winding we will analyze FC influence on efficiency ξ, depending on the number of turns w, which was varied from 1 up to 100 during calculations. Efficiency ξ of similar
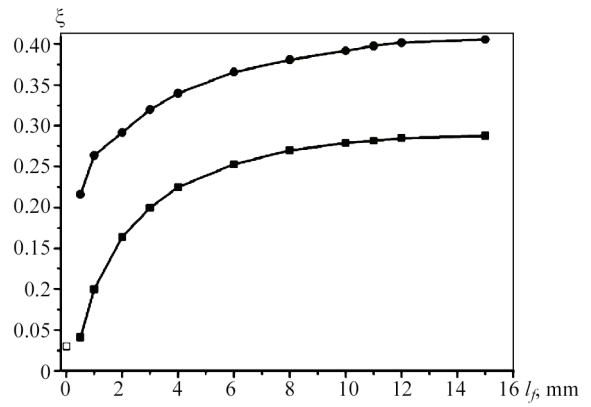
Figure 3. Design of the simplest ECP with one single-layer winding on FC

Figure 5. Dependence of efficiency ξ on FC length in case of mounting the winding at FC end (●), with an offset of 0.5 mm (■) and in the absence of FC (□)

windings of ECP without FC was also determined for comparison. Dependence of ξ coefficient on the number of turns was studied, when the winding is placed directly at the end of 10.0 mm long FC with initial magnetic permeability (MP) of the material μ = 100, 600, 1200, 2000 without shifting ($l_w = 0$). Calculations were conducted for working frequency of 10.0 MHz when mounting on a copper sample that corresponds to the conditions of investigation of efficiency ξ [18]. Dependencies of efficiency ξ on the number of turns w for coils without core and with FC with different initial MP μ are shown in Figure 4, *a*.

Derived dependencies show (Figure 4, *a*) that efficiency ξ for ECP with single-layer winding, mounted on FC, becomes significantly higher, compared to ECP without a core, depending on winding length (number of turns w), even at minimum value of FC material MP μ. At the same time, this effect depends on winding length, as efficiency ξ gradually decreases with its increase. Derived dependencies of efficiency ξ for MP μ = 100 and μ = 600 are rather close. Dependencies of efficiency ξ on the number of turns w (or winding length) for μ = 600, 1200 and 2000 are practically identical. This is confirmed by the dependence of efficiency ξ on initial MP μ of FC material (Figure 4, *b*). This dependence was calculated for a

single-layer coil, which consists of 25 turns, wound with 0.06 mm wire, placed with a shifting of 0.5 mm on FC of 1.2 mm diameter and 7.0 mm length. Results, presented in Figure 4, *b*, show that efficiency ξ increases from 0.24 up to 0.27 with increase of the initial MP μ from 100 to 2000. The greatest increase of efficiency ξ, however, is observed in the initial portion of the dependence, when MP has not yet reached value μ = 500. At further increase of MP μ, increase of efficiency ξ is insignificant.

The next dependencies (Figure 5) allow evaluation of the influence of FC length and winding position on it on ECP efficiency ξ. For this purpose, efficiency ξ was calculated for ECP, where the single-layer winding consists of 25 turns, wound with 1.2 mm wire. As indicated above, ECP of such a diameter are optimal to detect 2 mm long cracks. Calculations were conducted for core material MP μ = 500. Coefficients of efficiency ξ for parametric ECP with different FC length were calculated for a winding, placed at the end of FC without shifting ($l_{sh} = 0$), and for winding, mounted with shifting l_{sh} = 0.5 mm (Figure 3). Efficiency ξ of ECP with similar winding without FC was also calculated and was equal to approximately 0.025 (point □ in Figure 5).

Figure 4. Dependencies of efficiency ξ of single-layer parametric ECP on number of turns w in the absence of FC (■) and with FC with material MP μ = 100 (○) and μ ≥ 600 (Δ) (*a*) and on initial MP μ of FC material (*b*)

The given results show that FC application significantly increases the efficiency of parametric ECP. For windings placed at the end of FC, ξ coefficients are increased 7 times even for short FC 0.5 mm long. ECP efficiency ξ rises with increase of FC length. When a certain FC length is reached (close to 5 mm for this winding), increase of efficiency ξ becomes slower, and when FC length $l_f = 10.0$ mm is reached, it becomes close to the maximum value. These results show that it is rational to select FC length l_f in the range from 6.0 up to 10.0 mm. Here, efficiency of ECP windings mounted with an offset of 0.5 mm, decreases not as strongly as for short FC of the length smaller than $l_f = 2.0$ mm. For FC of length $l_f = 10$ mm shifting of the winding relative to FC end to distance $l_{sh} = 0.5$ mm decreases the efficiency ξ 1.45 times. Such losses can be considered acceptable. Note that such a shifting of the winding relative to FC working end prevents possible ECP failure through wear during scanning of EO surface. Therefore, a certain compromise during selection of winding shifting l_{sh} is justified. More over, these results allow evaluation of the possible changes in ECP characteristics, when part of FC wears in operation. It must be remembered that absolute value of ECP inductance also increases significantly with FC application.

3. OPTIMIZATION OF ELECTRIC AND DESIGN CHARACTERISTICS OF PARAMETRIC ECP

Investigations, presented in Sections 1 and 2, were used to design the basic parametric ECP for aviation industry of Ukraine, in keeping with the specifications of the main customers (SC Antonov, SC Ivchenko-Progress, PJSC Motor-Sich, etc.). Currently available range of FC was analyzed and taken into account during development. The main characteristics of basic ECP are given in Table 1.

SELECTION OF WORKING POINT
FOR SEPARATION OF THE INFLUENCE OF THE
DEFECT AND THE LIFT-OFF

ECP parameters given in Table 1, determine the impedance of inductive winding Z_w, provided it is placed at a distance from electrically conducting objects (in "air"). Let us consider the changes in electrical characteristics of basic parametric ECP, when placed on nonmagnetic structural materials with different specific electric conductivity (SEC). Inductance L and introduced resistance R_{in} of basic ECP (without cable) were calculated by the method of volume integral equations [11, 12, 19] at operational frequency of 2.0 MHz, when mounted on SS from nonmagnetic metal, the SEC σ of which was changed from 0.05

to 58.0 MS/m. Moreover, inductances of basic ECP without the cable, when mounted on SS with different SEC, were measured, using quality factor meter VM 560. Obtained results (Figure 6, *a*) show a good convergence of the calculation results with the experiment (within 5–8 %). Here, the inductance of basic ECP at operational frequency of 2 MHz decreases essentially in the range of SEC change up to 0.5 MS/m. At further increase of SEC in the range up to 5.0 MS/m, the speed of inductance rise with SEC increase becomes smaller. At further increase of SEC up to copper SEC value (58.0 MS/m) inductance L of ECP winding practically does not change. It allows substantiation of the possibility of using only two modes for ECFD: first — for testing low-conductivity nonmagnetic alloys (titanium alloys, austenitic steel) with SEC from 0.44 up to 2.4 MS/m; the second — for testing in a broader range from magnesium alloys (smallest SEC value of 5.8 MS/m) up to copper (58.0 MS/m). Such a wide range of SEC for the controlled alloys in the second mode can be ensured due to slight changes in basic ECP inductance within the range of SEC changes in these alloys (Figure 6, *a*). It significantly simplifies the design of self-generator ECFD.

With SEC increase, introduced resistance R_{in} of ECP winding first rises to a maximum at σ ≈ 0.2 MS/m, and then begins decreasing that corresponds to general regularities of the theory of eddy current technique as to changes in impedance components with SEC increase [1–6].

The influence of the defect and lift-off between ECP and EO surface can be separated by realization of the ""supercritical" mode (point "B" in Figure 7), which is in place with high values of generalized parameter $\beta = R\sqrt{\omega\sigma\mu\mu_0} > 5$; where: R is the equivalent radius of ECP winding; $\omega = 2\pi f$, where f is the operational frequency; $\mu_0 = 4\pi10^{-7}$ H/m is the magnetic constant; μ and σ are the relative MP and SEC of EO material.

Figure 7 shows that in the "supercritical" mode the changes of introduced resistance due to defect (D) and lift-off (L) have different sign, unlike the "subcritical"

Table 1. Characteristics of basic ECP

Characteristic	Value
FC diameter D_f, mm	1.2
FC height l_f, mm	7.0
Number of turns w	25
Wire diameter d_w, mm	0.06
FC material MP μ_f	500
Distance l_{sh}, mm	0.5
Number of layers	1
Winding resistance, Ohm	1.2
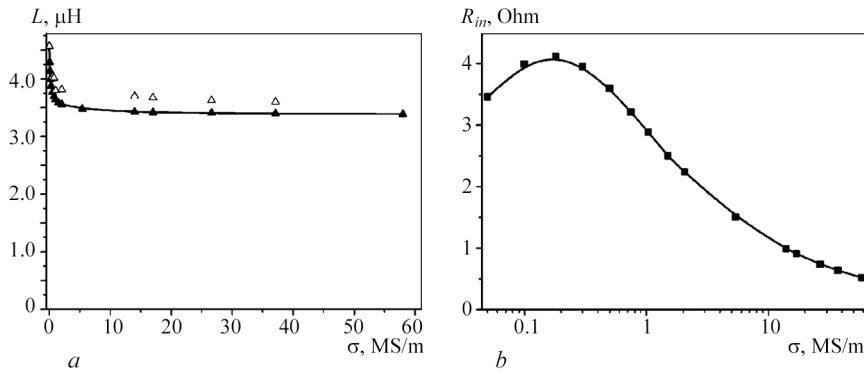
Figure 6. Dependence of inductance L (*a*) and introduced resistance (*b*) of basic ECP on SEC σ of EO material: ▲ and ■ — calculation; ∆ — experiment

mode (point A). The maximum point in Figure 6, *b* corresponds to the start of fulfillment of the condition of "supercritical" position of the working point of the introduced impedance hodograph, required to separate the influence of the defect and the lift-off. It means that for basic ECP at more than 2.0 MHz working frequencies the possibility of separation of the influence of the defect and the lift-off is realized even for low-conductivity titanium alloys with SEC in the range from 0.44 to 2.4 MS/m.

REDUCTION OF THE INFLUENCE
*OF PARASITIC COMPONENTS OF IMPEDANCE*

Equivalent circuit of parametric ECP, including the components for their connection to ECFD, can be presented in the form of three elements, connected in series. We will denote their impedance as follows: Z_w — impedance of ECP winding directly; Z_t — impedance of winding terminals and Z_c — impedance of the cable for ECP connection to ECFD. Impedance Z_w directly of ECP winding was analyzed in the previous section. Impedance of other elements, in particular, terminal impedance Z_t and connecting cable impedance Z_c are parasitic, as they do not participate in formation of a

useful signal from the defect, and their changes may lead to reduction of ECP quality factor on the whole and generation of additional interference. In self-generator or resonance ECFD these elements are part of the oscillatory circuit, so that they can significantly influence their operation and limit ECP interchangeability (Figure 8).

Let us consider in greater detail the parasitic components of ECP impedance, namely: terminal impedance Z_t and connecting cable impedance Z_c. Parasitic impedance Z_t can be inadmissibly large, as in parametric ECP with a small number of turns (25 in basic ECP) the terminal length is commensurate with the total length of winding turns. It leads to reduction of informative fraction of the components of parametric ECP impedance (active and inductive resistances), introduced by the defect. Here, ECP quality factor is also significantly reduced. It has an essential influence on their sensitivity in autogenerator and resonance operating modes. In order to reduce the influence of parasitic impedance Z_t of the terminals, a design of parametric ECP was proposed, into which a dielectric insert was incorporated, having two electrically conducting buses, the cross-sections of which are by an order of magnitude larger that those of winding wire (see Uchanin V.M., RybachukV.G., Kyrychenko I.I. Surface parametric eddy current probe. Patent of Ukraine 137775, 2019, Bull. No.21). Figure 9, *a* shows the design of parametric ECP for manual testing, where: *1* is the ECP casing; *2* is the winding; *3* is the connector; *4* is the dielectric insert; *5* are the electrically conducting buses; 6 are the terminals; 7 are
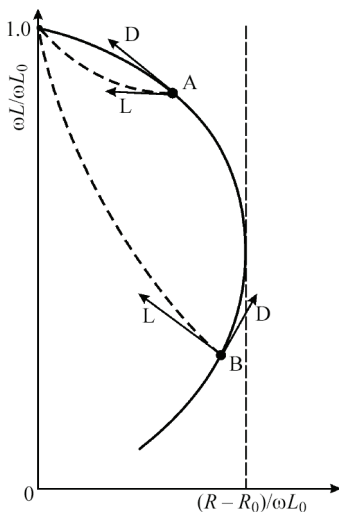
Figure 7. Influence of defect (D) and change of lift-off (L) on the hodograph of ECP impedance for the working point in the "subcritical" (point A) and "supercritical" (point B) modes [1]
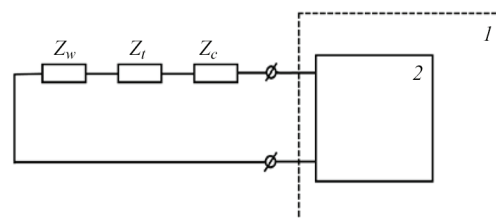
Figure 8. Equivalent circuit of parametric ECP: *1* — ECFD; *2* — oscillatory circuit
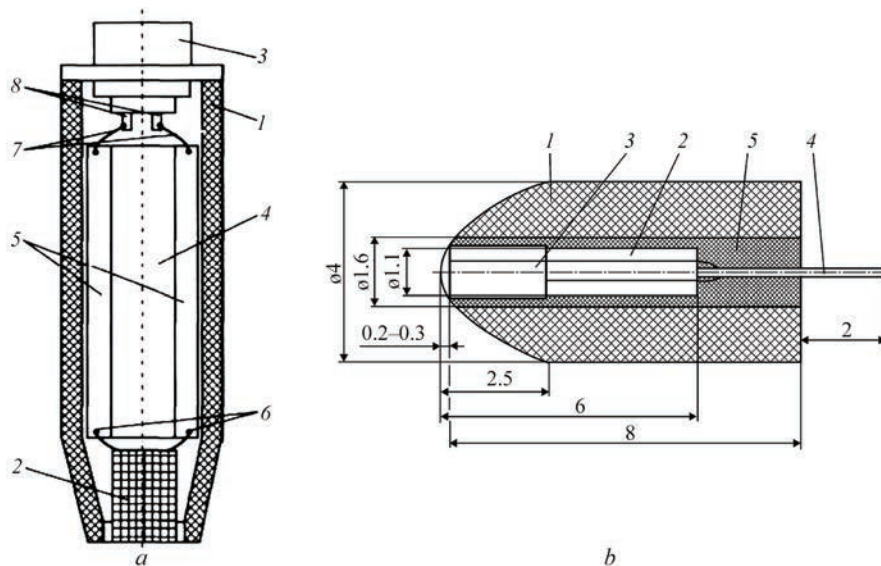
Figure 9. Designs of high-Q parametric ECP: a — ECP for manual testing; b — miniature ECP for testing difficult-of-access zones using a manipulator

the connecting wires; *8* are the connector contacts. Inductive winding terminals are connected to the ends of electrically conducting buses from the side of insert end face, adjacent to the winding, and terminals of the cable connector or the cable proper are connected to the ends of electrically conducting buses from the side of the opposite end face of the dielectric insert. It is better to place the electrically conducting buses from one side of the plate of the dielectric insert, as in this case their parasitic capacitance is significantly smaller.

In addition, these design features were used to create miniature ECP to detect defects on the inner surfaces of difficult-of-access cavities using manipulators. Design of miniature ECP (Figure 9, *b*) consists of a tubular polystyrol casing *1* of *4* mm diameter and *8* mm height, respectively, which contains FC *2* with winding *3* and dielectric insert *4* with electrically conducting buses. All the ECP elements are fastened in casing *1* using epoxy *5*. The protruding beyond the casing parts of electrically conducting buses of the dielectric insert are the contacts for ECP connection to ECFD cable. Testing showed that the *Q*-factor of such ECP is $Q = 0.53$, unlike ECP of a traditional design, for which $Q = 0.253$. Thus, the proposed technical solution allows increasing the quality factor of parametric ECP more than 2 times.

OPTIMUM SELECTION OF THE CONNECTING
CABLE FOR CONNECTION
OF PARAMETRIC ECP

As noted above, the characteristics of the cable for connection of the parametric ECP, also essentially influence ECFD operation. This is particularly true for self-generator and resonance ECFD, in which the cable impedance changes the resonance contour characteristics. Z_c values of the cable depend on its grade and cable length. In order to select the cable grade, its mechanical properties are analyzed, in particular flexibility and resistance to multiple bending during control operation performance. Cable length should be within 1–1.5 m for convenient scanning of EO surface by the operator under real production conditions. Due to that cable impedance Z_c cannot be reduced to such small values compared to winding impedance Z_w that it could be ignored. During cable selection it is important to ensure stable Z_c values during procedural manipulations and ECP interchangeability. The latter is particularly critical for self-generator ECFD of LEOTEST ECFD type, for which it is specified that the distributed capacitance of the connecting cable should be equal to 100 ± 5 pF. Depending on cable grade, not only the capacitance, but also other parameters, in particular specific attenuation (per a unit of length), are changed. In small diameter cables it reaches 0.4 dB/m. In thicker cables this parameter is essentially smaller and may drop to 0.05 dB/m, but they are not quite suitable for application, because of their low flexibility. Cable characteristics, in particular, their quality factor, essentially depend on the used materials. Materials based on polyethylene, polystyrene, and polytetrafluoroethylene are used for insulation. The central conductor of the radiofrequency cable can consist of one or several copper wires, tinned copper, copper with silver coating, etc. For optimal selection of the cable using quality factor meter of VM 560 type, electrical parameters of different cable variants of 1.5 m length were measured. The results are given in Table 2, where: R is the resistance; C is the capacitance; Q is the quality factor; L is the induc-

Table 2. Electrical characteristics of the cables (1.5 m length)

Cable type	R, Ohm	C, pF	Q	L, μH	ρ, Ohm	R_{eq}, Ohm
RK 50-1.5-11	0.24	121.0	6.0	0.23	40.3	242
RK 50-1.5-13	0.09	147.3	10.4	0.15	38.4	399
RK 50-2-11	0.25	168.0	7.0	0.19	33.7	236
RK 75-2-11	0.17	100.6	10.2	0.28	48.9	499
RK 75-2-13	0.20	97.9	10.8	0.34	58.5	632
RK 75-2-13A	0.18	99.0	10.6	0.31	63.5	673
Shielded twisted pair MGTF-0.14	0.41	110.0	12.0	0.79	95.3	1144
Shielded twisted pair MGShV-0.2	0.11	165.0	26.0	0.44	101.7	2644
Shielded wire MGShVE-0.2	0.14	257.0	7.5	0.90	54.8	411
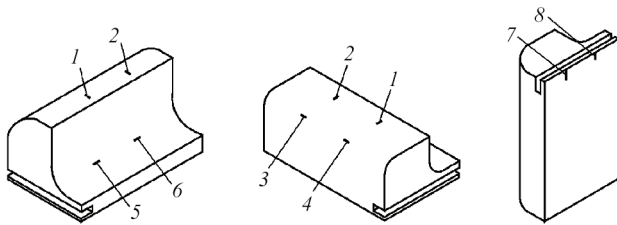
Figure 10. Appearance of SS with defects of SOP 5 type

tance; $\rho = \sqrt{L/C}$ is the wave resistance; $R_{eq} = \rho Q$ is the equivalent resistance.

Analysis of Table 2 leads to the following conclusions:

1. In the absence of stringent requirements as to cable length, all the grades of ratio-frequency cables with up to 100 pF specific capacitance and satisfactory quality factor can be used.

2. As to electrical parameters, cable of RK 75-2-11 grade looks the most suitable. Its application, however, is limited, because of high mechanical rigidity, which rises considerably at low temperatures.

3. Shielded wire pairs of MGTF-0.14, MGShV-0.2 and MGShVE-0.2 grades are hardly suitable for application by the totality of their electrical parameters.

4. Cables of RK-75-2-13 and RK 75-2-13A grades are optimal to manufacture longer (about 1.5 m cables) that is related to low values of specific capacitance.

5. Cables of grades RK 50-1.5-11 and RK 50-2-11 have relatively higher capacitance, lower quality fac-

tor, wave and equivalent resistance. Therefore, they can be used in the cases, when a relatively small cable length is admissible.

4. EXPERIMENTAL TESTING OF PARAMETRIC ECP: ANALYSIS OF SENSITIVITY AND POSSIBILITY OF SEPARATION OF THE INFLUENCE OF DEFECT AND LIFT-OFF CHANGE

The ECP presented above was studied using ECFD of EDDYCON type in the resonance mode. ECP was tested using standard specimen (SS) of SOP 5 type from aluminium, and titanium alloy and from ferromagnetic steel, respectively (Figure 10). Short slots of 2 mm length and up to 0.1 mm groove were made on SS surface by electric spark method. Slots of 0.2 and 0.5 mm depth were made on the surface of SS from an aluminium alloy, and slots of 0.5 mm and 1.5 mm depth were made on the SS from titanium alloy and steel. In addition to slots in SS flat part (defects *1*, *2* in Figure 10), slots were made on the cylindrical convex (defects *3*, *4* in Figure 10) and concave (defects *5*, *6* in Figure 10) regions of 6 mm radius. In addition, two defects of 0.5 and 1.0 mm length (defects *7*, *8* in Figure 10) were introduced in SS edge zone. Such SS allow evaluation of ECP sensitivity by defect depth and length in ferromagnetic steels and nonferromagnetic materials with different SEC for flat and curvilinear surfaces. The defectfree portion of these SS was also used to record the ECP signal from a change of lift-off. Looking ahead, we will note that
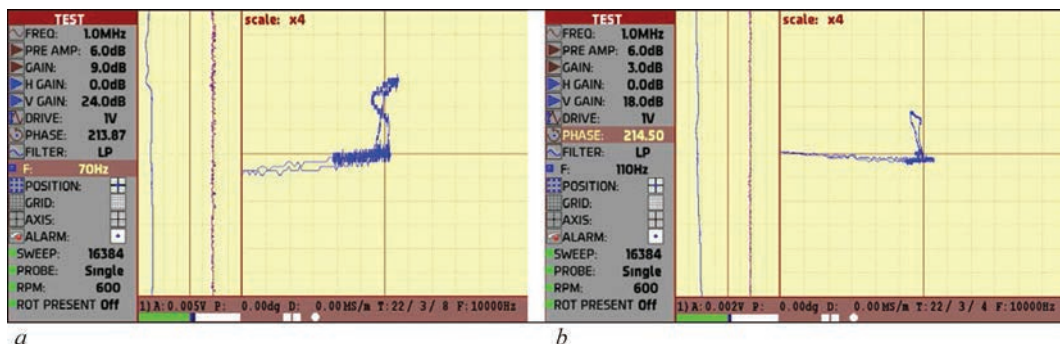
Figure 11. Signals of parametric ECP from a cracklike defect 2 mm long and 0.2 mm deep (*a*) and 0,5 mm (*b*) in aluminium alloy SS and from a lift-off change (*a*, *b*) at working frequency of 1.0 MHz
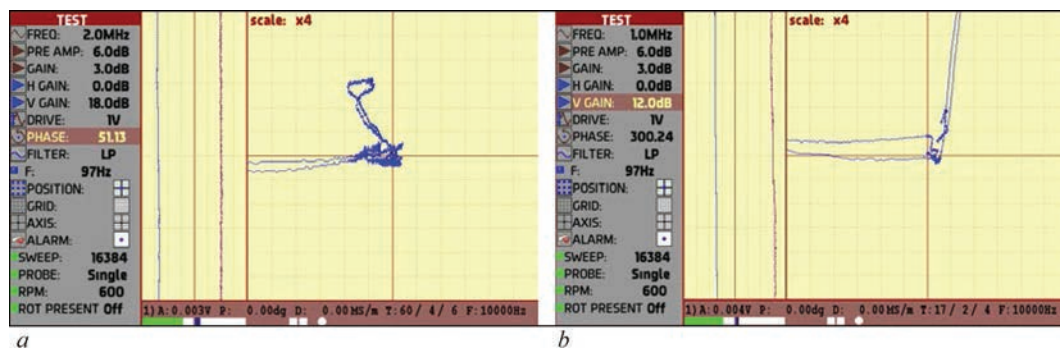
Figure 12. Signals of parametric ECP from a cracklike defect 2 mm long and 1.5 mm deep and from the change of lift-off in SS from titanium alloy (*a*) and from ferromagnetic steel (*b*)

basic ECP allowed reliable detection of all the defects in the above-mentioned SS, including defects on the convex and concave surfaces in the edge zone.

Results of testing parametric ECP to detect short cracks on SS from an aluminium alloy (Figure 11) demonstrated a sufficient sensitivity to defects 2 mm long and more than 0.2 mm deep with good separation of the signal from the lift-off and defect at operational frequency of 1.0 MHz. For this purpose, a methodological technique was used, when vertical sensitivity is higher than horizontal sensitivity (by 24 dB in Figure 11, *a*, and by 18 dB in Figure 11, *b*).

In order to test parametric ECP on titanium alloy SS, the operational frequency was increased up to 2 MHz, because of their essentially smaller SEC. Results of testing SS from a titanium alloy are given in Figure 12, *a*. Figure 12, *b* shows the results of testing SS from ferromagnetic steel at 1 MHz operational frequency. Here, vertical sensitivity is also greater than the horizontal one (by 18 dB in Figure 12, *a*, and by 12 dB in Figure 11, *b*).

Results presented in Figure 12, *a*, *b* show that ECP ensures detection of cracks longer than 2.0 mm in titanium alloys and ferromagnetic steels with the possibility of effective debugging from the influence of lift-off change. Note that the lower sensitivity by depth for defects in titanium alloys, compared to sensitivity to defects in aluminium alloys is known, and it is attributable to their essentially lower SEC. For ferromagnetic steels the sensitivity by depth is often limited by a significantly higher risk of interference, reducing which requires either additional magnetization or application of selective ECP [21].

CONCLUSIONS

1. Results of investigations and developments, associated with optimization of the design of parametric ECP to detect surface defects, were generalized.

2. Selection of ECP diameter was substantiated, depending on the smallest length of cracks to be detected. It is shown that in order to detect more than 2 mm long cracks, application of ECP with windings mounted on

FC of 1.2 mm diameter is optimal. To detect short cracks more than 1 mm long an ECP was developed with winding mounted on FC of 0.75 mm diameter.

3. The influence of FC parameters (length, magnetic permeability and winding shifting from FC end) on the efficiency of parametric ECP was analyzed for their optimization.

4. Conditions of separation of the influence of the defect and lift-off were analyzed by interpretation of signals in a complex plane, and the possibility of their separation was shown for all the nonmagnetic structural alloys.

5. A design of parametric ECP is presented, which allows improving their quality factor more than 2 times, and the issue of optimal selection of the connecting cable for ECP connection to ECFD is considered.

6. Testing of basic parametric ECP was conducted, which confirmed its high sensitivity to short cracks more than 2 mm long with reliable separation of the influence of the defect and lift-off.

REFERENCES

1. Dorofeev, A.L., Kazamanov, Yu.G. (1980) *Electromagnetic flaw detection*. Moscow, Mashinostroenie [in Russian].
2. Gerasimov, V.G., Pokrovsky, A.D., Sukhorukov, V.V. (1992) *Non-destructive testing.* In: 5 Books. Book 3: Electromagnetic testing. Moscow, Vysshaya Shkola [in Russian].
3. Libby, H.L. (1971) *Introduction to Electromagnetic Non-destructive Test Methods*, New-York, Wiley-Interscience.
4. García-Martín, J., Gómez-Gil, J., Vázquez-Sánchez, E. (2011) Non-destructive techniques based on eddy current testing. *Sensors*, **11**, 2525–2565. DOI: https://doi.org/10.3390/s110302525
5. AbdAlla, A.N. Faraj, M.A., Samsuri, F., Rifai, D., Ali, K., Al-Douri, Y. (2019) Challenges in improving the performance of eddy current testing: Review. *Meas. Control*, **52**, 46–64. DOI: https://doi.org/10.1177/0020294018801382
6. Rao, B.P.C. (2011) Eddy current testing: Basics. *J. of Non-Destructive Testing & Evaluation*, 10(**3**), 7–16.
7. Hagemaier, D.J. (1991) Application of crack detection to aircraft structures. In: *Fatigue Crack Measurement: Techniques and Applications.* Eds by K.J. Marsh, R.A. Smith and R.O. Ritchie. Warley (UK): EMAS, 419–455.
8. Uchanin, V. (2021) Enhanced eddy current techniques for detection of surface-breaking cracks in aircraft structures. *Transact. on Aerospace Research*, 262(**1**), 1–14. DOI: https://doi.org/10.2478/tar-2021-0001.e, ISSN 2445-2835

9. Uchanin, V. (2007) Specific features of the space distribution of the signal of an eddy-current converter caused by cracks of different lengths. *Materials Sci.,* 43(**4**), 591–595. DOI: https://doi.org/10.1007/s11003-007-0068-2

10. Sobolev, V.S. Shkarlet, Yu.M. (1967) *Surface and screen sensors*. Novosibirsk, Nauka [in Russian].

11. Dyakin, V.V., Sandovsky, V.A. (1981) *Theory and calculation of surface eddy current converters.* Moscow, Nauka [in Russian].

12. Sabbagh, H.A., Sabbagh, L.D., Bowler, J.R. (1988) A model of ferrite-core probes over composite workpieces. *Review of Progress in Quantitative Nondestructive Evaluation*, **7A**, 479–486. New York, Plenum Press.

13. Sabbagh, L.D., Hedengren, K.H., Hurley, D.C. (1991) Interaction of flaw with a ferrite-core eddy current probe: Comparison between model and experiment. *Review of Progress in Quantitative Nondestructive Evaluation*, **10A**, 883–888. New York, Plenum Press.

14. Beda, P.I. (1970) Examination of signal of surface sensor depending on change of sizes and location of crack type defects. *Defektoskopiya*, **1**, 62–68 [in Russian].

15. (2000) EN 13860-2: *Non-destructive testing — Eddy current examination — Equipment characteristics and verification.* Pt 2: Probe characteristics and verification. European Committee for Standardization.

16. Capobianco, T.E., Splett, J.D., Iyer, H.K. (1990) Eddy current probe sensitivity as a function of coil construction parameters. *Research in Nondestructr. Eval.*, **2**, 169–186.

17. Capobianco, T.E. (1987) Field mapping and performance characterization of commercial eddy current probes. *Review of Progress in Quantitative Nondestructive Evaluation*, **6A**, 687–694. New York, Plenum Press.

18. Uchanin, V. (2012) Invariant efficiency parameter of eddy-current probes for nondestructive testing. *Materials Sci.,* 48(**3**), 408–413. DOI: https://doi.org/10.1007/s11003-012-9520-z

19. Dunbar, W.S. (1985) The volume integral method of eddy current modeling. *J. Nondestruct. Eval.*, 5(**1**), 9–14.

20. (1996) *User's Guide for VIC-3D: An Eddy Current NDE Code. Version 2.4.* USA, Bloomington, Sabbagh Associates, Inc.

21. Uchanin, V., Nardoni, G. (2020) Eddy current detection of cracks in ferromagnetic steel structures. In: *The Fundamentals of Structural Integrity and Failure*. Ed. by Richard M. Wilcox, Nova Sci. Publishers, NY, USA, 193–221.

ORCID

V.M. Uchanin: 0000-0001-9664-2101

CORRESPONDING AUTHOR

V.M. Uchanin
G.V. Karpenko Physico-Mechanical Institute
of the NASU
5 Naukova Str., 79060, Lviv, Ukraine.
E-mail: vuchanin@gmail.com

SUGGESTED CITATION

JOURNAL HOME PAGE